Effects of atmospheric stability conditions on heat fluxes from small water surfaces in (semi-)arid regions

Abbasi, Ali; Annor, Frank Ohene; van de Giesen, Nick

DOI
10.1080/02626667.2017.1329587

Publication date
2017

Document Version
Final published version

Published in
Hydrological Sciences Journal

Hydrological Sciences Journal

ISSN: 0262-6667 (Print) 2150-3435 (Online) Journal homepage: http://www.tandfonline.com/loi/thsj20

Effects of atmospheric stability conditions on heat fluxes from small water surfaces in (semi-)arid regions

Ali Abbasi , Frank Ohene Annor & Nick van de Giesen

To cite this article: Ali Abbasi , Frank Ohene Annor & Nick van de Giesen (2017) Effects of atmospheric stability conditions on heat fluxes from small water surfaces in (semi-)arid regions, Hydrological Sciences Journal, 62:9, 1422-1439, DOI: 10.1080/02626667.2017.1329587

To link to this article: http://dx.doi.org/10.1080/02626667.2017.1329587

Accepted author version posted online: 11 May 2017.
Published online: 02 Jun 2017.

HYDROLOGICAL SCIENCES JOURNAL – JOURNAL DES SCIENCES HYDROLOGIQUES, 2017
VOL. 62, NO. 9, 1422–1439
https://doi.org/10.1080/02626667.2017.1329587

Effects of atmospheric stability conditions on heat fluxes from small water surfaces in (semi-)arid regions

Ali Abbasi [a,b], Frank Ohene Annor[a,c] and Nick van de Giesen[a]

[a]Faculty of Civil Engineering and Geosciences, Water Resources Section, Delft University of Technology, Delft, The Netherlands; [b]Faculty of Engineering, Civil Engineering Department, Ferdowsi University of Mashhad, Mashhad, Iran; [c]Civil Engineering Department, Kwame Nkrumah University of Science and Technology, Kumasi, Ghana

ABSTRACT

Atmospheric stability conditions over the water surface can affect the evaporative and convective heat fluxes from the water surface. Atmospheric instability occurred 72.5% of the time and resulted in 44.7 and 89.2% increases in the average and maximum estimated evaporation, respectively, when compared to the neutral condition for a small shallow lake (Binaba) in Ghana. The proposed approach is based on the bulk-aerodynamic transfer method and the Monin-Obukhov similarity theory (MOST) using standard meteorological parameters measured over the surrounding land. For water surface temperature, a crucial parameter in heat flux estimation from water surfaces, an applicable method is proposed. This method was used to compute heat fluxes and compare them with observed heat fluxes. The heat flux model was validated using sensible heat fluxes measured with a 3-D sonic anemometer. The results show that an unstable atmospheric condition has a significant effect in enhancing evaporation alongside the sensible heat flux from water surfaces.

ARTICLE HISTORY
Received 4 June 2016
Accepted 22 December 2016

EDITOR
A. Castellarin

ASSOCIATE EDITOR
A. Viglione

KEYWORDS
evaporation; small reservoirs; atmospheric boundary layer; stability condition; semi-arid region

1 Introduction

Small reservoirs, or lakes, in (semi-)arid regions, especially in developing countries, constitute a substantial fraction of the regionally available water resources. These reservoirs provide water to improve food security, stimulate agricultural economy and income diversification through irrigating farms, and make possible livestock farming, particularly in rural areas where most of their inhabitants rely on rainfed agriculture (Poussin *et al.* 2015). While there are many benefits associated with these small reservoirs, their storage efficiency is significantly affected by the primary source of water loss, evaporation (Liebe *et al.* 2009). In arid and semi-arid areas, annual evaporation losses from lakes and reservoirs account for up to 50% of the accumulated stored water (Mugabe *et al.* 2003, Gokbulak and Ozhan 2006, Martínez-Granados *et al.* 2011, Gallego-Elvira *et al.* 2012, Fowe *et al.* 2015). Therefore, accurate estimation of evaporation is critically important to assess the reliability of using small reservoirs to enhance water security for all direct and indirect economic activities (e.g. irrigated crops, livestock feed, fish processing, brick making, etc.) enabled by these water sources, mainly in the dry season (Liebe 2009). In spite of the importance of accurate estimations in regional-scale hydrology and water resources management, evaporation is perhaps the most difficult of hydrological cycle components to estimate because of the existence of complex interactions at the water surface–atmosphere system (Singh and Xu 1997a). Shallow and small lakes usually experience high variability in atmospheric boundary layer stability conditions due to their fast heating and cooling by the surrounding land. Apart from this, due to generally low wind speeds over small water surfaces (Verburg and Antenucci 2010), unstable atmospheric conditions can last for a long time (Rouse *et al.* 2003), which results in enhanced sensible and latent heat fluxes (Brutsaert 1982). As small inland water bodies are influenced significantly by the atmospheric boundary layer stability conditions, estimating evaporative fluxes from their surface is challenging.

The available methods for estimating evaporation from water surfaces use two general approaches: (i) direct measurement of evaporation, such as the evaporation pan method (Fu *et al.* 2004, 2009) and eddy covariance (EC) flux measurements (Stannard and Rosenberry 1991, Blanken *et al.* 2000, Assouline *et al.* 2008, McGloin *et al.* 2014a, b); and (ii) calculating (indirect) evaporation by using measured meteorological parameters. The indirect

CONTACT Ali Abbasi a.abbasi@tudelft.nl

methods can be put into four categories, mainly through the approach they use in estimating evaporation using meteorological inputs: (i) the water budget (balance) method; (ii) the energy balance and combination methods (Gianniou and Antonopoulos 2007, Rosenberry *et al.* 2007); (iii) the aerodynamic or mass transfer method (Singh and Xu 1997b); and (iv) the radiation- and temperature-based methods (Xu and Singh 2000, 2001). The water balance method is simple in theory but difficult in practice (Finch and Calver 2008). In this method, evaporation is computed as the change in volume of water stored and the difference between the inflows and outflows of the lake. The relative importance of the terms depends on the hydrological and physiographical settings (Finch and Calver 2008). Direct measurement of evaporation at the air–water interface is often very expensive and has to be designed carefully to obtain reliable data. The energy balance and combination methods have been seen to be reliable in providing precise estimations of evaporation (Delclaux *et al.* 2007, Rosenberry *et al.* 2007, Ali *et al.* 2008), but these methods need a wide range of datasets as input parameters such as net radiation, conduction heat flux and heat storage of the water body (Gallego-Elvira *et al.* 2012, Vidal-López *et al.* 2012) to estimate evaporation. In most of these methods, the model parameters used are specific for the given water body under the prevailing surrounding environment and climate, and are valid only for the specific ranges of parameters (reservoir size, air and water surface temperature difference, humidity, atmospheric conditions, etc.) used in the designed experiment (Vinnichenko *et al.* 2011). This means that these coefficients may not provide satisfactory estimations for other regions (Sartori 2000).

In this study, evaporation from small water bodies is estimated using an improved mass transfer method considering the effects of atmospheric stability conditions. This method needs moderate input data and correlates evaporation to vapour pressure deficit between the surrounding air and the water surface. Although a wide range of empirical mass transfer approaches have been applied by researchers, in most of these methods a linear function of wind speed, referred to as "wind function" with constant coefficients, was applied to estimate evaporative heat fluxes from the water surface. Applying some of the common mass transfer methods to estimate evaporation from the study lake (Lake Binaba in Ghana) revealed that the differences between the values estimated from different methods were very high, and therefore choosing a suitable method was difficult. Furthermore, developing a method that includes time-varying effects of atmospheric conditions on the transfer coefficient (or wind function, which correlates the evaporation to the vapour pressure deficit between the water surface and the atmosphere) would be very promising, especially for small lakes under conditions of data (or measurement) scarcity.

To calculate the vapour pressure deficit between a water surface and the air above it, which is required in the mass transfer method, both water surface temperature and air temperature should be available. As in most small lakes (e.g. those in the study region), micrometeorological parameters measured over the water surface are rarely available, and developing a method to estimate heat fluxes from the water surface using only land-based stations would be practical. Investigation of the correlation matrix of (measured) water surface temperature values shows that the temperature can be estimated from standard micrometeorological parameters measured over surrounding land. Applying this approach for two small lakes in the study region, a method was developed to estimate water surface temperature using land-based measurements.

The developed approaches (both water surface and heat flux models) were used to estimate heat fluxes from a small water body in northern Ghana. As the method developed in this study uses only land-based measurements, which are commonly available near the lakes, it could easily be applied to estimate heat fluxes from small water surfaces based on the available measurements and the conditions of the small reservoirs in this area. In addition, this approach with some minor modification (for instance in the equation used to calculate the water surface temperature) is generalizable and cost effective and could be used for other similar inland water bodies.

To determine the effects of atmospheric stability on estimated heat fluxes, sensible and latent heat fluxes were estimated during the study period (23 November 2012 to 22 December 2012) using the proposed improved mass transfer (bulk aerodynamic) method for a small shallow lake, Lake Binaba in Ghana. Using the proposed (aerodynamic) method and standard micrometeorological variables (air temperature, wind speed, relative humidity and air pressure) measured over the area around the lake, the sensible and latent heat fluxes were calculated taking into account the stability conditions of the atmospheric boundary layer over the water surface. To determine the influence of atmospheric stability conditions on the estimated heat fluxes from the water surface, the components and parameters were adjusted for the study site conditions. The mass

transfer coefficient was adjusted using stability functions to include the atmospheric stability conditions in estimating evaporation. In addition, the time-dependent atmospheric conditions and water surface characteristics were used in the model to improve the algorithm developed for estimating the evaporation.

Considering the importance of heat flux (e.g. evaporation) estimation from small water surfaces and the difficulties in doing that, the main aims of the present study are: (I) to develop a model for calculating water surface temperature in small lakes using only standard land-based measurements, to close the gap in data needed for heat flux estimation; (II) to develop a generalizable and cost-effective method to estimate heat fluxes from inland water surfaces; (III) to consider the effects of atmospheric stability conditions on heat fluxes from water surfaces; and (IV) to analyse the heat flux data footprint and data-filtering issues of measured heat fluxes to use them in model validation. To evaluate the performance of the model against observed values of sensible heat flux, some quantitative metrics, including root mean square error (RMSE), mean absolute error (MAE), index of agreement (d) and the bias values were applied. In addition, the performance of the model was investigated under different atmospheric stability conditions. From these metrics, the results show that the simulated sensible heat fluxes are in good agreement with the observed ones.

2 Description of study site and data collection

The Upper East Region of Ghana (UER) has more than 160 small shallow reservoirs with surface areas ranging from 0.01 to 1.0 km^2 (Annor *et al.* 2009). These small reservoirs have the advantage of being operationally efficient with their flexibility, closeness to the point of use, and requirement for few parties for management (Keller *et al.* 2000). The studied lake is a small shallow reservoir located in this region. Lake Binaba (10°53′20″ N, 00°26′20″W) is an artificial lake, used for water supply, irrigation, livestock watering, construction, fishing, domestic uses and recreation. A natural stream has been dammed, storing and providing water for all these uses in Binaba, a small town in the sub-humid region of Ghana (van Emmerik *et al.* 2013). The lake surface area is around 306 000 m^2, with average and maximum depths of 1.1 and 4.0 m, respectively. The length of the lake (x-direction) is around 900.0 m and its width (y-direction) is 600.0 m (Fig. 1).

To measure the sensible heat flux and the atmospheric stability conditions over the lake, a 3-D sonic anemometer was installed at 1.90 m above the water surface. Measurements (and the computed variables) taken by the sonic anemometer included turbulent fluctuations of vertical wind, sonic temperature, sensible heat flux, momentum flux, Obukhov length (or equivalent stability parameter), the source areas of 80% of the integrated flux (footprint), etc. The installed sonic

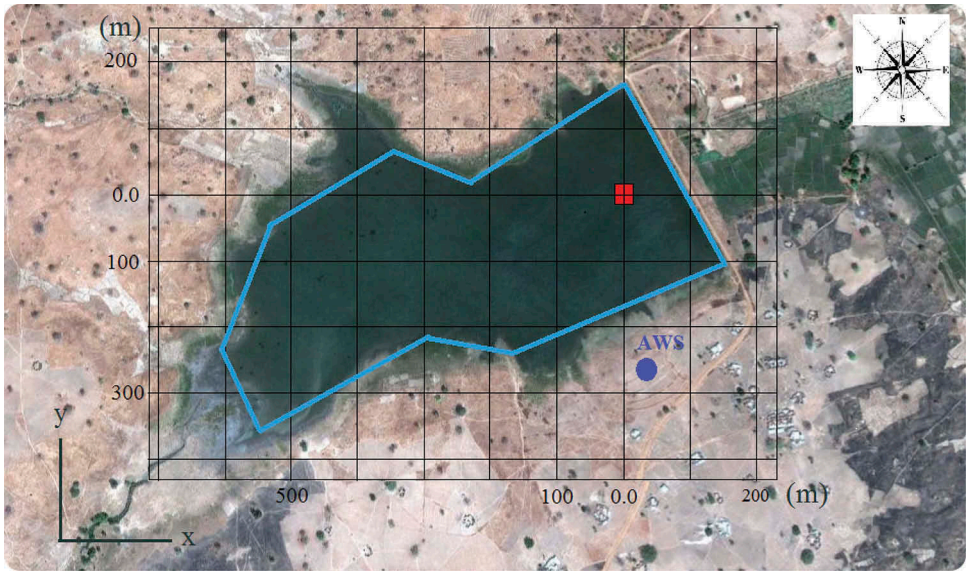

Figure 1. Shape of Lake Binaba and its surroundings (Google Earth). Locations of the floating sonic anemometer and land-based automatic weather station (AWS) are shown by a square (red) and dot (blue), respectively. The blue outline shows the area over the water surface used in the footprint analysis of heat flux data, as explained in Section 9.1. (Lengths in m.)

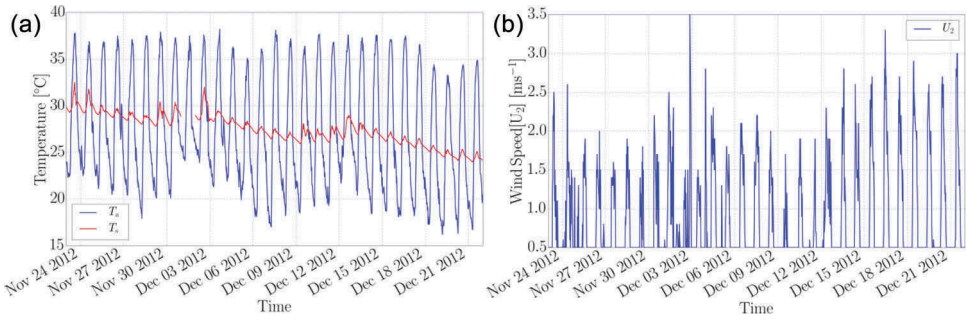

Figure 2. Measured (a) water surface and air temperatures and (b) wind speed at 2 m above land surface during the simulation period. Wind speed is averaged over 30-min intervals.

anemometer recorded measurements (e.g. sensible heat flux) over the water surface at 10 Hz and accumulated over 30-min intervals. The raw eddy correlation data were processed by Alteddy software (version 3.90) (Elbers 2002, 2016). As processing the raw eddy correlation data is beyond the goals of this manuscript, the reader is referred to Annor *et al.* (2016) for more details and challenges on processing such data over small water surfaces. After processing the raw eddy correlation data, footprint analysis was executed to select only the measurements that represent the water surface (Section 7.1). Finally, the filtered and processed data (sensible heat flux) were used to validate the computed sensible heat fluxes using the proposed model.

In addition, the atmospheric parameters needed as input to the model were measured. The standard climatic parameters of air temperature, relative humidity, wind speed and wind direction were recorded around the lake (over land) at a height of approx. 2.0 m above the ground (Fig. 1). The automatic weather station (AWS) installed on the land was provided with a solar radiation sensor (model PYR, Decagon Devices, USA; ±5%) for solar radiation flux density measurement (in W m^{-2}), a humidity/temperature sensor (model VP-4, Decagon Devices, USA; ±2% and ±0.25°C for humidity and temperature, respectively) for air humidity and air temperature measurement, and a sonic anemometer (model DS2, Decagon Devices, USA; ±3% and ±3° for wind speed and wind direction, respectively) to measure wind speed and its direction. The microclimatic parameters (air temperature, relative humidity, wind speed and its direction) were averaged on 30-min intervals and used as input values in the proposed model.

As water surface temperature is a crucial parameter in calculating heat fluxes (particularly for sensible heat), it was measured during the study period. The water surface values were measured by HOBO tidbit v2 temperature loggers with a nominal accuracy of ±0.2° C. The measured water surface temperature values were used in the model to estimate heat fluxes. Moreover, these measured values were used to validate the calculated water surface temperature values by using the standard meteorological parameters measured in the AWS installed over the surrounding land (Section 5).

During the study period (23 November 2012–22 December 2012) the air temperature fluctuated from 18.0 to 40.0°C, with an average of 28.7°C, while the water surface temperature varied between 24.0 and 32.5° C, with an average of 27.5°C. Figure 2(a) shows the diurnal changes of water surface temperature and air temperature, with daily variations of approximately 10.0°C. The wind speed values recorded by the land-based AWS are shown in Figure 2(b), with the southwestern direction being the most dominant at a maximum speed of 3.5 m s^{-1}. Since the wind speed values were averaged on 30-min intervals, instantaneous wind speed may be larger.

3 Bulk aerodynamic method

The study of sensible and latent heat fluxes from water surfaces has produced a large body of literature. One of the most suitable methods with moderate input data is the bulk-aerodynamic transfer method. The bulk-aerodynamic approach, which is based on a Dalton-type equation and Fick's first law of diffusion, can be used to estimate sensible heat and latent heat fluxes through a fixed boundary layer such as that developed over the free water surface of a reservoir (Dingman 2002). It is based on the concept of mass transfer theory, which states that the diffusion of heat and water vapour into the atmosphere moves from where its concentration is larger to where it is smaller at a rate proportional to the spatial gradient of that concentration. This method is straightforward because it relies on relatively routine measurements of wind speed, air temperature, relative humidity and water surface temperature. Except for the water surface temperature, all the required input

parameters are measured over the surrounding land. In addition, for water surface measurements, as they are not available in most cases, a model as developed in this study can be used. Assuming that the boundary layer over a smooth water surface is similar to that over a rough water surface, the following equations can be used to calculate sensible and latent heat fluxes (Hicks 1975):

$$H = \rho_a C_p C_H U_z (T_{ws} - T_a) \quad (1)$$

$$E = \rho_a \lambda C_E U_z (q_s - q_z) \quad (2)$$

where H is sensible heat flux (W m^{-2}), E is latent heat flux (W m^{-2}), ρ_a is the density of air (kg m^{-3}), C_p is the specific heat of air (≈1005 J kg^{-1} K^{-1}), C_H and C_E are (bulk) transfer coefficients for sensible heat and latent heat, respectively (–), U_z is wind speed at height z above the water surface (m s^{-1}), T_a is air temperature (°C), T_{ws} is water surface temperature (°C), λ is the latent heat of vaporization of water (J kg^{-1}), q_s is the saturated specific humidity at water surface temperature (kg kg^{-1}) and q_z is the specific humidity (kg kg^{-1}).

The density of air (ρ_a) can be calculated as follows:

$$\rho_a = 100 \times \left(\frac{P_{atm}}{R_a (T_a + 273.16)} \right) \quad (3)$$

with

$$R_a = 287.00[1 + 0.608 q_z] \quad (4)$$

where P_{atm} is atmospheric pressure (Pa) and R_a is the gas constant for moist air (J kg^{-1} K^{-1}). The latent heat of vaporization of air (λ) is a function of temperature and can be given by:

$$\lambda = 2.501 \times 10^6 - 2361 \times T_a \quad (5)$$

where T_a is in °C. Specific humidity for water surface temperature and air temperature can be obtained from:

$$q_s = \frac{0.6108 e_{sat}}{P_{atm}} \quad (6)$$

$$q_z = \frac{0.6108 e_a}{P_{atm}} \quad (7)$$

where e_{sat} is saturated vapour pressure at T_{ws} (in kPa), e_a is actual vapour pressure (kPa) and e_s is saturated vapour pressure at T_a (kPa):

$$e_{sat} = 0.6108 \exp\left[\frac{17.269 T_{ws}}{T_{ws} + 237.3} \right] \quad (8)$$

$$e_a = e_s \times \frac{RH}{100} \quad (9)$$

$$e_s = 0.6108 \exp\left[\frac{17.269 T_a}{T_a + 237.3} \right] \quad (10)$$

To estimate latent heat flux in m s^{-1} the following equation can be used:

$$E^* = \frac{E}{\rho_w \lambda} \quad (11)$$

where ρ_w (in kg m^{-3}) is water density, given by (Henderson-Sellers 1986):

$$\rho_w = 1000 \times \left(1 - 1.9549 \times 10^{-5} |T_{ws} - 3.84|^{1.68}\right) \quad (12)$$

Examining the above equations indicates that the main input parameters required for this model to estimate heat fluxes are: water surface temperature, T_{ws} (°C); air temperature, T_a (°C); wind speed measured at height z (typically 2.0 or 10.0 m) above the surrounding land, U_z (m s^{-1}); relative humidity, RH (%); and air pressure, P_{atm} (Pa). These parameters can be measured by land-based weather stations installed around the water surface (Fig. 1). Although the water surface temperature is needed to compute the atmosphere stability parameter, its measurements are rarely available in the case of small shallow lakes. However, for the study lake, water surface measurements are available to close the gap in the input data, especially for water surface temperature. A correlation approach was developed in this study to estimate this variable from micrometeorological parameters measured over the nearby land (Section 5).

4 Estimating transfer coefficients

Heat and mass transfer coefficients are influenced by atmospheric stability conditions over the lake and, therefore, could be affected by gradients of temperature and humidity over the water surface as well as wind speed values. In this section, an algorithm is proposed to calculate the transfer coefficients adjusted to the site-specific measurements and modify them according to the stability conditions over the water surface. The proposed framework is based on the algorithms commonly used for estimating sensible and latent heat fluxes from oceans and large lakes (Fairall *et al.* 1996, Zeng *et al.* 1998, Renfrew *et al.* 2002). These methods have rarely been used to estimate evaporation from small lakes in arid and semi-arid regions. The proposed algorithm is able to: (i) take into account the roughness lengths of momentum, water vapour and temperature (Brutsaert 1982) in the transfer coefficients; (ii) adjust the air density, water density, water vapour pressure and other parameters included for local conditions; and (iii) start with neutral transfer coefficients and then adjust them for different stability conditions.

4.1 Determining the atmospheric stability conditions

The atmospheric stability conditions over the water surface have a significant impact on the sensible and latent heat fluxes from the water body. When the skin (water surface) temperature (T_{ws}) is higher than air temperature (T_a), the atmospheric boundary layer is unstable and convective. The air and water surface temperature (skin temperature) differences can be used as a measure of atmospheric stability (Derecki 1981, Croley 1989). In an unstable atmospheric boundary layer, commonly the water surface temperature is higher than the air temperature. However, using the differences between the absolute water surface temperature and the air temperature is not strictly correct, since the effects of wind speed and relative humidity play key roles in the atmospheric stability.

To be considered on heat fluxes, the atmospheric stability conditions need to be estimated, and one of the most popular frameworks for this is the Monin-Obukhov similarity theory (MOST), which relates changes in vertical wind speed gradient, temperature and water vapour concentration. Obukhov length (L in m) is the parameter used to define atmospheric stability; L is linked to a dimensional analysis of the turbulent kinetic energy (TKE) equation and the ratio of the shearing and buoyancy effects (Stull 1988). Monin and Obukhov (1959) suggested that the vertical changes in mean flow parameters and turbulence characteristics in the atmospheric boundary layer may depend only on the surface momentum flux or measured friction velocity (u_*), sensible heat (H) and latent heat (E) fluxes and height (z):

$$L = \frac{-u_*^3 \rho_a T_{av}}{\kappa g \left[\left(\frac{H}{C_p}\right) + 0.61 \frac{(T_a + 273.16)E}{\lambda}\right]} \quad (13)$$

The Obukhov length (L) is an indicator of the ratio of the turbulent kinetic energy reduction due to wind mixing and the atmospheric stratification growth due to the heat flux (Brutsaert 1982). In this equation, ρ_a is air density (kg m^{-3}), u_* is friction velocity (m s^{-1}), κ is the von Karman constant (≈0.41), T_{av} is virtual air temperature (K), H is sensible heat flux (W m^{-2}), E is latent heat flux (W m^{-2}), C_p is the specific heat of air (J kg^{-1} K^{-1}), g is the gravitational acceleration (≈9.81 m s^{-2}), T_a is air temperature (°C) and λ is latent heat of vaporization of water (≈2264.76 × 10^3 J kg^{-1}). According to the values of L, the stability conditions are usually classified as reported in Table 1. In most cases, the non-dimensional stability parameter ($\zeta = z/L$, where z is height above the water surface in m) can be used as an indicator for atmospheric stability (Table 1).

Table 1. Stability classification of atmospheric boundary layer (ABL) (Barthlott *et al.* 2007).

		Characteristics	Stability class
$L < 0$	$\zeta < 0$	Unstable	Unstable and convective ABL, enhancing the vertical heat fluxes
$L > 0$	$\zeta > 0$	Stable	Stable boundary layer, reducing the vertical heat fluxes
$L \to +\infty$	$\zeta = 0$	Neutral	Atmospheric transfer coefficients are equal to their neutral values
$L \to -\infty$	$\zeta = 0$	Neutral	Atmospheric transfer coefficients are equal to their neutral values

To consider the effect of water vapour concentration, L is calculated using the virtual temperature instead of absolute temperature to take into consideration the fact that the density of moist air is less than that of dry air (Monteith and Unsworth 2008). The virtual air temperature (T_{av}) can be calculated as:

$$T_{av} = (T_a + 273.16)[1 + 0.61 q_z] \quad (14)$$

and similarly, the virtual temperature of saturated air at the water surface (T_{wsv}) is given by:

$$T_{wsv} = (T_{ws} + 273.16)[1 + 0.61 q_s] \quad (15)$$

and the virtual air–surface temperature difference is written as:

$$\Delta T_v = T_{wsv} - T_{av} \quad (16)$$

where T_{av} is the virtual air temperature (in K), and T_{wsv} is the virtual temperature of saturated air at the water surface (in K), ΔT_v is the virtual air–surface temperature difference (in K), T_a and T_{ws} are air temperature and water surface temperature, respectively (°C), q_s is saturated specific humidity at water surface temperature (kg kg^{-1}), which can be calculated using Equation (6), and q_z is the specific humidity of air (kg kg^{-1}) calculated from Equation (7).

4.2 Neutral transfer coefficients

Comparing the actual (including the stability effects) and neutral (assuming neutral conditions, N) heat fluxes from small water surfaces gives a clear idea of the effects of atmospheric stability conditions on heat fluxes. In this study, first the neutral heat fluxes were computed and then adjusted for stability conditions. Neutral transfer coefficients for momentum and heat fluxes in the atmospheric boundary layer are determined from:

$$C_{DN} = \left(\frac{u_*}{U_z}\right)^2 = \left(\frac{\kappa}{\ln(z/z_{0m})}\right)^2 \quad (17)$$

$$C_{EN} = \frac{\kappa^2}{\ln(z/z_{0m})\ln(z/z_{0q})} = \frac{\kappa C_{DN}^{1/2}}{\ln(z/z_{0q})} \quad (18)$$

Under near-neutral conditions the transfer coefficients for sensible heat (C_{HN}) and latent heat (C_{EN}) are assumed equal (Zeng *et al.* 1998, Verburg and Antenucci 2010);

$$C_{HN} = C_{EN} \quad (19)$$

where C_{DN} is a neutral drag (momentum) coefficient (0), C_{EN} is a neutral latent heat transfer coefficient (–), C_{HN} is a neutral transfer coefficient for sensible heat (–), κ is the non-dimensional von Karman constant (≈0.41), z is the measurement height of climate variables (2.0 m above the land surface), z_{0m} is the roughness length of momentum (m), z_{0q} is the roughness length for water vapour (m) and g is the gravitational acceleration (9.81 m s^{-2}). Air shear velocity (friction velocity, u_*, in m s^{-1}) is obtained from:

$$u_* = \left(C_D U_z^2\right)^{(1/2)} = \frac{\kappa U_z}{\ln(z/z_{0m})} \quad (20)$$

and the functional form of Smith (1988) is implemented to estimate momentum roughness length, z_{0m} (Smith 1988, Zeng *et al.* 1998):

$$z_{0m} = \alpha\left(\frac{u_*^2}{g}\right) + \beta\left(\frac{\nu}{u_*}\right) \quad (21)$$

where α represents the Charnock constant (α = 0.013) (Zeng *et al.* 1998) and β is a constant (β = 0.11). The roughness length of humidity (and temperature) is given by the functional form of Brutsaert (1982):

$$\ln\frac{z_{0m}}{z_{0q}} = b_1 \mathrm{Re}_*^{1/4} + b_2 \Rightarrow z_{0q} = z_{0m}\exp\left(b_1 \mathrm{Re}_*^{1/4} + b_2\right) \quad (22)$$

where b_1 = – 2.67 and b_2 = 2.57 are constant and Re_* is the roughness Reynolds number calculated by:

$$\mathrm{Re}_* = \frac{u_* z_0}{\nu} \quad (23)$$

The kinematic viscosity of air, ν (m^2 s^{-1}), can be calculated using:

$$\nu = \frac{\mu}{\rho_a} \quad (24)$$

where the dynamic viscosity of air, μ (N s m^{-2}) is computed from a linear function of air temperature, T_a (°C) (Verburg and Antenucci 2010):

$$\mu = 4.94 \times 10^{-8} T_a + 1.7184 \times 10^{-5} \quad (25)$$

In neutral conditions the roughness length for temperature (z_{0h}) is assumed to be the same as that for water vapour (z_{0q}) (Zeng *et al.* 1998, Verburg and Antenucci 2010):

$$z_{0h} = z_{0q} \quad (26)$$

As mentioned previously, in the proposed algorithm the neutral transfer coefficients are estimated at the first step and then modified for the atmospheric stability conditions. To start the computation procedure, an initial value for friction velocity (u_*) is needed. Therefore, the computation was started with an initialized u_* using the equation of Amorocho and DeVries (1980):

$$u_* = U_{10}\left(0.0015\left[1 + \exp\left[\frac{U_{10} + 12.5}{1.56}\right]^{-1}\right] + 0.00104\right)^{-2} \quad (27)$$

where U_{10} is wind speed at 10.0 m above the water surface, which can be estimated from U_z by (Schertzer *et al.* 2003, Verburg and Antenucci 2010):

$$U_{10} = U_z\left(\frac{10}{z}\right)^{1/7} \quad (28)$$

after obtaining z_{0m} from:

$$U_{10} = U_z\frac{\ln(10/z_{0m})}{\ln(z/z_{0m})} \quad (29)$$

Using this initial value of u_* with Equations (20) and (21), a simple iteration loop is performed to calculate the momentum roughness length and get the desired convergence criteria (within 0.001% of the previous value). After calculating the z_{0m} using this algorithm, the neutral transfer coefficients can be estimated.

4.3 Modifying transfer coefficients for atmospheric stability conditions

To consider the effects of atmospheric stability on heat fluxes, the heat and mass transfer coefficients should be modified regarding the atmospheric stability conditions. This is done using stability functions (Dyer 1967, Businger *et al.* 1971, Brutsaert 1982). There are many stability functions (Ψ) for stable and unstable conditions of the atmospheric boundary layer. In this study, the following stability functions were used:

- for stable conditions ($\zeta < 0$), all transfer stability functions for momentum, heat and mass (Ψ_M, Ψ_T and Ψ_E, respectively) are assumed to be equal (Dyer 1967, Businger *et al.* 1971) and given by:

$$\Psi_M = \Psi_T = \Psi_E = \begin{cases} -5\zeta & \text{if} \quad 0 < \zeta \leq 0.5, \\ 0.5\zeta^{-2} - 4.25\zeta^{-1} - 7\ln\zeta - 0.852 & \text{if} \quad 0.5 < \zeta \leq 10, \\ \ln\zeta - 0.76\zeta - 12.093 & \text{if} \quad \zeta > 10, \end{cases} \tag{30}$$

- for an unstable atmospheric boundary layer ($\zeta < 0$) the equations below could be used:

$$\Psi_M = \ln\left[\frac{(1+x^2)}{2}\right] + 2\ln\left[\frac{(1+x)}{2}\right] - 2\arctan(x) + \frac{\pi}{2} \tag{31}$$

$$\Psi_T = \Psi_E = 2\ln\left[\frac{1+x^2}{2}\right] \tag{32}$$

$$x = (1 - 16\zeta)^{1/4} \tag{33}$$

Using the atmospheric stability functions, the modified transfer coefficients can be written as:

$$C_D = \frac{\kappa^2}{[\ln(z/z_{0m}) - \Psi_M]^2} \tag{34}$$

$$C_E = \frac{\kappa^2}{[\ln(z/z_{0m}) - \Psi_M] \times [\ln(z/z_{0q}) - \Psi_E]} = \frac{\kappa C_D^{1/2}}{[\ln(z/z_{0q}) - \Psi_E]} \tag{35}$$

$$C_H = C_E \tag{36}$$

5 Estimating water surface temperature

In Section 3, the proposed approach for computing heat fluxes from water surfaces was explained. As can be seen, water surface temperature is a crucial parameter for sensible heat flux estimation. In addition, this parameter is required in advance to determine the atmospheric stability conditions for modifying the transfer coefficients (Section 4.3). However, for most inland water surfaces, especially small shallow ones in developing regions (countries), due to the logistical difficulties and economic issues in operating measurements over lakes, water surface temperature measurements are rarely available. In order to address this issue, a simple correlation model was used in this study. This model contains only micrometeorological parameters measured over land. As water surface temperature and standard meteorological parameters were available for the study period, a correlation matrix was established to find the main variables influencing the water surface temperature. The correlation coefficients between the water surface temperature and micrometeorological variables measured on land are presented in Table 2. As shown in Table 2, water surface temperature is mainly influenced by air temperature (T_a), relative humidity (RH) and incoming shortwave radiation (R_s), whereas the effect of wind speed, which mostly was low, could be ignored.

Table 2. Correlation matrix of (measured) water surface temperature values (bold row) in Lake Binaba with micro-meteorological parameters measured at the nearby land station.

Parameter	T_a (°C)	T_{ws} (°C)	U_2 (m s^{-1})	RH (%)	R_s (W m^{-2})
Air temperature (T_a)	1.000	0.458	0.529	−0.503	0.617
Water surface temperature (T_{ws})	**0.458**	**1.000**	**−0.006**	**0.300**	**0.130**
Wind speed (U_2)	0.529	−0.006	1.000	−0.467	0.708
Relative humidity (RH)	−0.503	0.300	−0.467	1.000	−0.578
Incoming shortwave radiation (R_s)	0.617	0.130	0.708	−0.578	1.000

After evaluating the different regression models to find the best fit to the measured values (using R software), the following equation was obtained:

$$T_{ws} = [2.187 \times T_a - 0.0631 \times {T_a}^2 + 0.001 \times {T_a}^3] + [0.006 \times R_s] + [0.377 \times RH - 0.005 \times RH^2] - 6.159; R^2 = 0.69 \tag{37}$$

where T_{ws} is water surface temperature (°C), T_a is air temperature (°C), R_s is incoming shortwave radiation (W m^{-2}) and RH is relative humidity (%).

To test the performance of the water surface temperature model, it was applied to another small lake in the study area, Lake Winkogo (10°42′48″N, 00°51′32″W), which is around 60.0 km away from Lake Binaba and, hence, their meteorological conditions are assumed to be the same. Similarly to Lake Binaba, the water surface temperature values and micrometeorological parameters measured over the surrounding land were available for Lake Winkogo (Annor *et al.* 2016).

Several evaluation measures for the performance of the water surface temperature model for both lakes Binaba and Winkogo are presented in Table 3. According to the evaluation measures presented in Table 3, the calculated water surface temperature values are in satisfactory agreement with the measured

Table 3. Evaluation of water surface temperature model performance. The model was validated for two similar lakes in the study area, Lake Binaba and Lake Winkogo. RMSE: root mean square error; MAE: mean absolute error; E: Nash-Sutcliffe efficiency coefficient; R^2: coefficient of determination; *d*: index of agreement.

Study lake	RMSE (°C)	MAE (°C)	*E*	R^2	*d*	Bias
Lake Binaba	1.029	0.850	0.65	0.71	0.88	−0.27
Lake Winkogo	1.582	1.302	0.45	0.58	0.80	−0.60

ones (Ali *et al.* 2015) and can be used in the estimation of heat fluxes from water surfaces (Section 3).

6 Model algorithm

In Equation (13), the Obukhov length (L) is a function of sensible (H) and latent (E) heat fluxes. Therefore, the stability functions are functions of sensible and latent heat fluxes over the water surface. The calculation procedure is initiated with neutral transfer coefficients for momentum, heat and mass (C_{DN}, C_{HN} and C_{EN}, respectively), followed by the neutral sensible and latent heat fluxes (H_N and E_N). Utilizing the neutral values, an iteration loop on L is established. In each iteration, air shear velocity (u_*), roughness lengths for momentum, temperature and water vapour (z_{0m}, z_{0h}, z_{0q}), modified transfer coefficients (C_D, C_H, C_E), sensible (H) and latent (E) heat fluxes are recalculated and applied to recalculate L and the stability functions (Ψ). These iterations are continued until L converges to within 0.0001% of the previous value of L. The framework of the model is depicted in Figure 3.

7 Model verification and validation

The main advantage of the new model developed in this study is to estimate both the evaporative heat flux and the sensible heat flux from small water surfaces. This model needs only standard micrometeorological parameters measured over land surrounding the inland water surface. In addition, water surface temperature can be used in the model either from measurements or from the proposed approach (as described in Section 5). For Lake Binaba, besides the standard meteorological parameters over the land, sensible heat fluxes were measured over the water surface during the study period using a 3-D sonic anemometer (Section 2). The observed sensible heat fluxes were used to validate the estimated convective heat fluxes from the water surface. Regarding the footprint of heat fluxes over the water surface, the measured heat fluxes should be filtered before being used in model validation.

7.1 Heat flux data filtering

Due to the non-sufficient (finite) dimensions of Lake Binaba in wind direction, to be sure that the fluxes come only from the water surface, the heat flux data

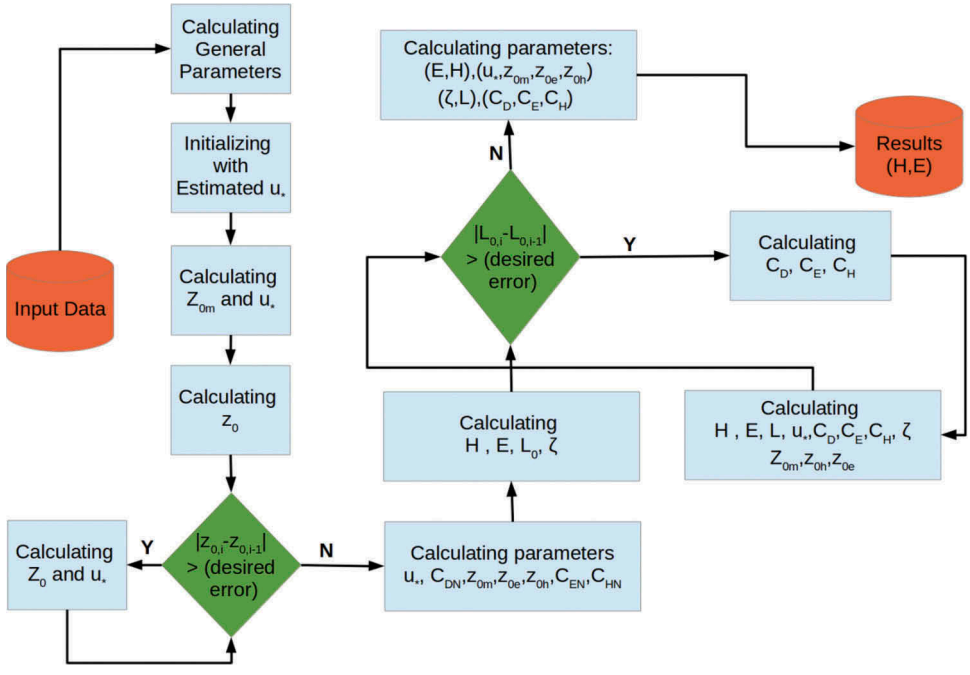

Figure 3. Proposed framework to estimate heat fluxes from water surface considering atmospheric stability conditions.

taken over the water surface had to be processed before being used in the validation process. The measured fluxes represent the upwind area fluxes, which are referred to as the footprint (FP). The dimensions and location of the measured heat flux footprints depend on the height of measurement, wind speed and its direction, surface properties and atmospheric stability conditions (Vesala *et al.* 2008). For small lakes with limited dimensions (e.g. Lake Binaba with less than 500 m) in the predominant wind direction, footprint analysis of heat flux measurements is a crucial concept. To select reliable fluxes that represent the fluxes from only the water surface, the following steps were used to filter the sensible heat flux measurements (after processing the raw data as mentioned in Section 2):

(1) Different ranges for wind direction were defined. For these ranges, the upwind distances, X_{ud} (in m), that include only the water surface were determined according to the geometry of the lake and its shape. The extent of this area, including only fluxes coming from the water surface, is shown in Figure 1 (blue outline).
(2) Using the prepared Python code, for each range of wind direction, and using the values of X_m and X_{ud} (determined in Step 1), the data points where $X_m \leq X_{ud}$ were extracted. Here, X_m (in m) is the source area (distance) of 80% of the integrated flux (footprint). According to Kljun *et al.* (2015), in most cases 80% of the footprint area includes the main impact of the measurement (it should be noted that 100% of the footprint area is infinite). X_m was computed by Alteddy software (version 3.90) and applied here for sensible heat data filtering for validation of the model.
(3) For the selected time frame from the filtered heat flux data, the heat flux footprint area (length) was calculated. For footprint prediction (FPP), the method developed by Kljun *et al.* (2015) for footprint parameterization was used (Fig. 4).

After data filtering, 559 (of 1392) half-hourly heat flux data points (43% of the initial dataset) remained for model validation. To investigate the model performance, the remaining data points were classified according to the atmospheric stability conditions using the ratio of z/L (or ζ where z is the height of measurement (m), L is Obukhov length (m) and $\zeta = z/L$ is the stability parameter (–)). The dataset properties used in this study are summarized in Table 4.

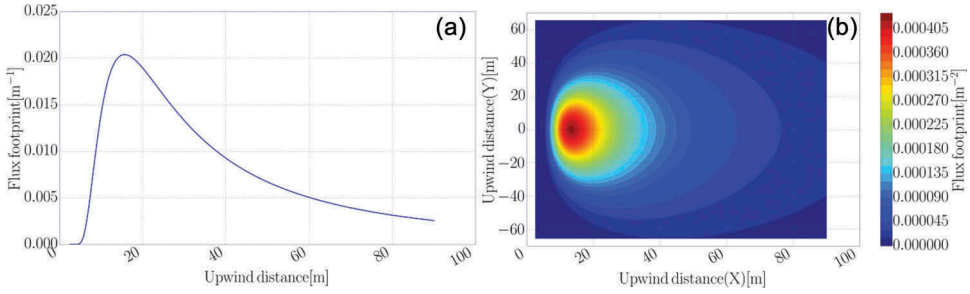

Figure 4. Footprint representations for the selected time frame (24 November 2012 at 19:30 h) in the study period. At this time frame the atmosphere was unstable, with L = –1.05 m; h (atmospheric boundary layer height) = 1930.7 m; u^* = 0.043 m s^{-1}; measurement height 1.90 m above water surface. The sonic anemometer is located at (0,0) m and the x-axis points towards the main wind direction: (a) footprint length estimate in main wind direction (1-D); and (b) footprint contour lines (2-D)

Table 4. Atmospheric stability condition in relation to measured heat flux data, with stability conditions for different datasets (F: filtered, NF: non-filtered). EC-NF: initial data point; EC-F: filtered data using proposed algorithm; M-Tws-Obs-NF, F: dataset using measured water surface temperature; M-Tws-Mod-NF, F: dataset using the simulated water surface temperature. Due to the lack of some input parameters (e.g. water surface temperature) the number of data points is less than the initial number of data points.

Dataset	Total data		Stable condition		Unstable condition	
	Number of points	Percentage	Number of points	Percentage	Number of points	Percentage
EC-NF	1327	100	366	27.58	961	72.42
EC-F	559	100	4	0.72	555	99.28
M-Tws-Obs-NF	1287	100	433	33.64	854	66.36
M-Tws-Obs-F	552	100	25	4.53	527	95.47
M-Tws-Mod-NF	1328	100	438	32.98	890	67.02
M-Tws-Mod-F	559	100	23	4.11	536	95.89

7.2 Validating the calculated sensible heat fluxes

As mentioned in Section 7.1, the filtered measured values of sensible heat flux from the sonic anemometer installed over the water surface were used to validate the model. The validation process was carried out to check the performance of the proposed model in different stability conditions. In Table 5 the measures of model performance are presented. According to the suggestion of Legates and McCabe (1999), to assess the performance of the model, four common quantitative evaluation criteria, namely, the root mean square error (RMSE), mean absolute error (MAE), index of agreement (*d*) and the bias (Bias) were used in this study. The values of the index of agreement (*d*) vary between 0.0 and 1.0, where 0.0 indicates no agreement and 1.0 represents perfect agreement for measured and estimated values (Legates and McCabe 1999, Ali *et al.* 2015).

Table 5. Calculated metrics of model (of heat flux calculation) performance for calculated sensible heat fluxes for different atmospheric stability conditions: RMSE: root mean square error; MAE: mean absolute error; *d*: index of agreement; Bias: bias. Different datasets are presented: Tws-Obs-30m: using observed water surface temperature values at 30-min intervals; Tws-Mod-30m: using calculated water surface temperature values at 30-min intervals; Tws-Obs-H: using hourly observed water surface temperature values; Tws-Mod-H: using hourly calculated water surface temperature values.

Dataset	Stability condition	RMSE (°C)	MAE (°C)	*d*	Bias
Tws-Obs-30m	Total data	10.40	6.29	0.54	−3.22
	Stable condition	15.24	13.45	0.47	−13.46
	Unstable condition	10.12	5.95	0.49	−2.74
Tws-Mod-30m	Total data	11.63	9.8	0.49	−9.50
	Stable condition	16.32	14.3	0.48	−14.30
	Unstable condition	11.38	9.61	0.47	−9.29
Tws-Obs-H	Total data	8.73	5.82	0.64	−3.71
	Stable condition	14.44	12.73	0.49	−12.73
	Unstable condition	8.18	5.34	0.60	−3.08
Tws-Mod-H	Total data	11.30	9.71	0.51	−9.49
	Stable condition	15.69	13.66	0.50	−13.66
	Unstable condition	10.97	9.46	0.47	−9.23

In Figure 5 comparisons of simulated and observed sensible heat fluxes from the water surface for stable and unstable atmospheric conditions are shown. The number of points in Figure 5(a) is small due to the filtering of measured sensible heat fluxes over the water surface (Section 7.1). After filtering the observed heat flux data (regarding the footprint values explained above), approximately all validation data (99%) belong to unstable atmospheric conditions and, therefore, validating the results for stable conditions is not accurate. However, as shown in Table 4, for most of the time (72.5%) the atmosphere is unstable over Lake Binaba. This means that if the model worked well in unstable conditions, it would cover most times and conditions available over the water surface. The performance of the model, as shown in Figure 5(b) and Table 5, is satisfactory according to the evaluation parameters. To investigate the performance of the model for all atmospheric stability conditions (especially for stable conditions) collecting long-term heat flux measurements (including sufficient stable and unstable conditions after data filtering) over the water surface as well as microclimate variables on land is crucial.

8 Model results and discussion

The proposed approach was applied to Lake Binaba in Ghana, for the study period 23 November 2012 to 22 December 2012. The input data to the model were provided by the on-ground AWS on the shore of the water body, as shown in Figure 1. The effects of atmospheric stability conditions on the transfer coefficients

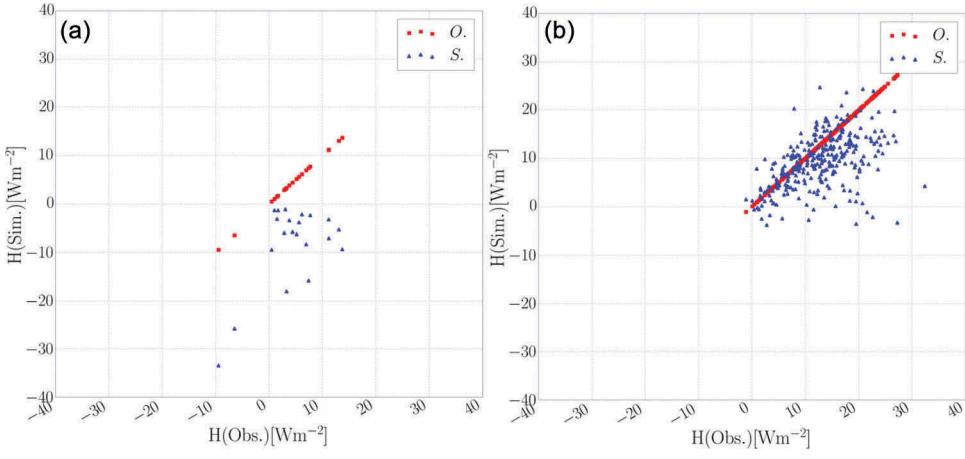

Figure 5. Comparison of simulated (Sim.) and observed (Obs.) sensible heat flux values over the water surface: (a) for atmospheric stable conditions and (b) for unstable atmospheric conditions. Squares (red) correspond to the 1:1 relationship.

and consequent heat fluxes from the water surface are discussed below.

8.1 Atmospheric stability

According to the Monin-Obukhov similarity theory (MOST), the stability parameter ζ can be used as an indicator of atmospheric stability; ζ depends on both the difference between the air and water surface virtual temperatures (ΔT_v) and horizontal wind speed. The value of $|\zeta|$ is large when wind speed is low. The ζ values computed for the study period show that the atmosphere was unstable in 72.5% of the study period at Lake Binaba (Table 4).The stability parameter (ζ or z/L) is usually unknown in most small lakes. Applying the proposed method, the value of L and, consequently, the stability parameter (ζ) can be computed and the atmospheric stability conditions can be indicated to apply the correct stability functions (Section 4.3).

8.2 Roughness lengths

The average roughness lengths of momentum and heat (or water vapour) are 5.51×10^{-5} m and 1.49×10^{-4} m, respectively. Figure 6(a) illustrates that the roughness length of momentum (z_{0m}) decreases for velocities up to 2.5 m s^{-1}, and for higher values of horizontal wind speeds (U_z > 2.5 m s^{-1}) its values increase gradually with wind speed. However, the trend of the heat (or water vapour) roughness length is different. The z_{0h} ($=z_{0q}$) does not vary significantly for wind speeds greater than 2.5 m s^{-1}, as shown in Figure 6(b).

Comparing the computed roughness lengths over the water surface shows that, unlike for the land surfaces, the heat (and water vapour) roughness length is larger than the momentum roughness length. For small lakes with low to moderate wind speeds ($U_2 \leq 5$ m s^{-1}), the water surface can be considered as a smooth surface. Unlike land surfaces (rough surfaces), for smooth surfaces z_{0q} and z_{0h} are larger than z_{0m}. Over rough surfaces (such as land areas) the heat (z_{0h}) and water vapour (z_{0q}) roughness lengths are considerably smaller than the momentum roughness length (z_{0m}) (Brutsaert 1982). These large differences in roughness lengths can be related to the different mechanisms for momentum and heat or water vapour transfer. Over rough surfaces, momentum transfer is enhanced by the effective drag, including local pressure gradients beside the viscous shear. The heat and water vapour transfer are controlled primarily by molecular diffusion (Brutsaert 1982). At lower wind speeds, the momentum exchanges over the water surface (smooth surface) are mainly affected by non-atmospheric factors such as swell on the water surface (Vercauteren 2011). However, the interaction between a turbulent atmosphere and an inland water surface (specifically for small shallow lakes) is complex and includes a number of complicated physical processes and, hence, the prediction of z_{0m} as well as z_{0h} and z_{0q} over the inland water surfaces is still subject to some uncertainty (Brutsaert 1982).

8.3 Transfer coefficients

Figure 7(a) shows the relationships between wind speed and neutral transfer coefficients. As can be seen from Figure 7(a), the average of the neutral drag coefficients is 1.60×10^{-3}. This value decreases for wind speeds up to 2.0 m s^{-1} and increases approximately linearly for higher wind speeds (U_2 > 2 m s^{-1}). The general trend of the neutral heat (or water vapour) transfer coefficient (with an average value of 1.76×10^{-3}) is the same as the drag coefficient, but its value decreases for wind speeds up to 3.0 m s^{-1} (this point is 2.0 m s^{-1} for drag coefficient). For wind speeds greater than 2.0 m s^{-1} it increases at a very smooth rate, less than the change rate of the neutral drag coefficient.

Using the stability functions to adjust the transfer coefficients increased the average of the drag coefficient

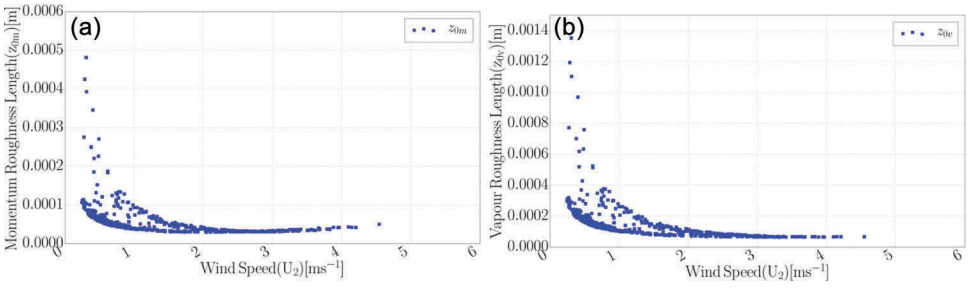

Figure 6. Relationship between the horizontal wind speed (measured over the surrounding land) and (a) momentum roughness length, and (b) heat (or water vapour) roughness length.

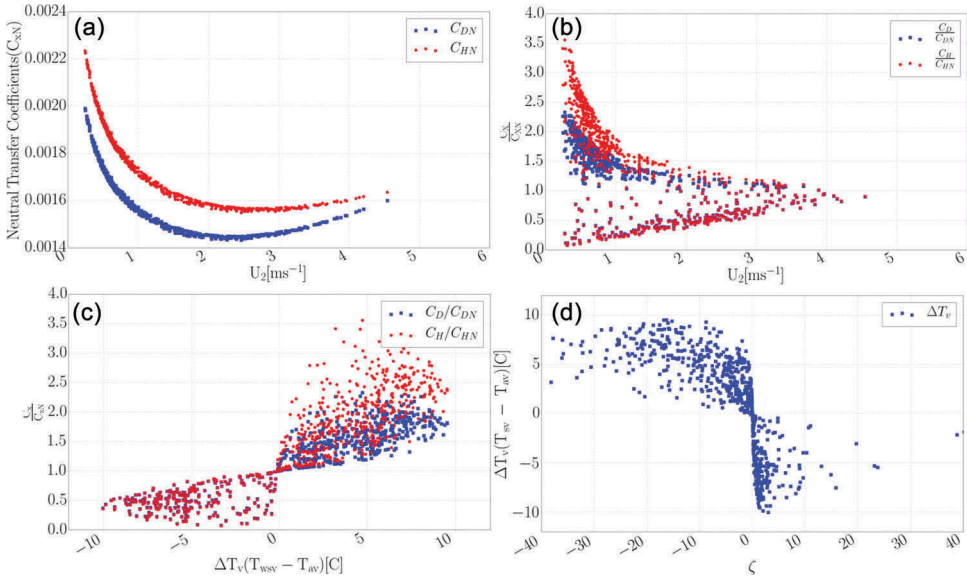

Figure 7. Relationship between wind speed values and (a) neutral transfer coefficients; (b) changes of ratio of transfer coefficients to their neutral values; (c) effect of virtual air–surface temperature difference on the transfer coefficients; and (d) relationship between virtual air–surface temperature difference and stability parameter values.

and heat (or water vapour) transfer coefficients by 25.9 and 48.3% to 2.02 × 10^{-3} and 2.61 × 10^{-3}, respectively. The effect of stability conditions on the transfer coefficients is largest for low wind speeds (as shown in Fig. 7 (b)) and for large values of (virtual) air–water surface temperature difference (ΔT_v or ΔT) (where $\zeta < 0$, as shown in Fig. 7(c)), which happen in unstable atmospheric boundary layers (Fig. 7(d)). This effect enhances the transfer coefficients and consequently the sensible and latent heat fluxes from the water surface. The modified transfer coefficients for a non-neutral atmosphere converge to neutral values (C_{DN}, C_{HN}) with an increase in wind speed, with ζ converging to zero (Fig. 8(a) and (b)).

The ratios of the stability adjusted transfer coefficients to the neutral coefficients C_E/C_{EN} and C_D/C_{DN} were larger than 1.0 when ΔT_v was positive and the atmospheric boundary layer was unstable (Fig. 7(c)). The rate of change of the modified transfer coefficients

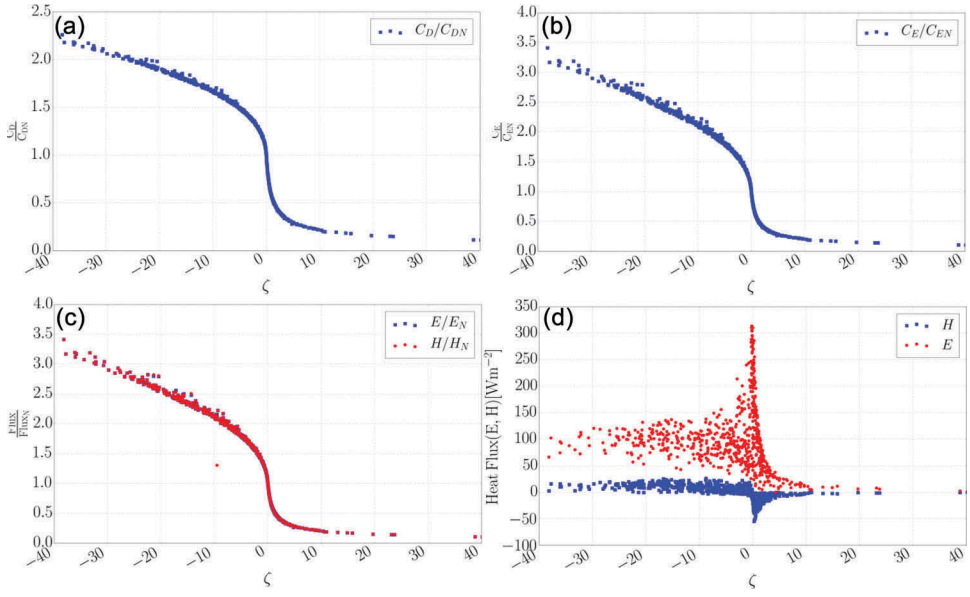

Figure 8. Relationship between the stability parameter and (a) ratio of momentum transfer coefficient to corresponding neutral values; (b) ratio of heat (or water vapour) transfer coefficient to corresponding natural values; (c) ratio of heat fluxes to their neutral values; and (d) sensible and latent heat fluxes.

with ζ was fast for values of ζ close to zero and attenuated for increasing $|\zeta|$ (Fig. 8(a) and (b)). The ratio C_E/C_{EN} in unstable conditions was larger than the ratio C_D/C_{DN} and, therefore, the effects of atmospheric stability conditions were higher for water vapour (heat) transfer than for the drag forces.

8.4 Sensible and latent heat fluxes

In this study, heat fluxes from small inland water surfaces were calculated taking into account atmospheric stability conditions. With this aim, the heat (C_H) and mass (water vapour) transfer coefficients (C_E) were modified to take the stability conditions into consideration. When stability functions were used to calculate sensible heat and latent heat fluxes from the water surface, the average estimated latent (evaporation) heat flux increased by 44.7% compared with estimates using the neutral atmospheric boundary layer (Fig. 8(c)). This rate is lower than the increase in the average value of C_E, which was 48.3% because the atmospheric stability effect on C_E is largest at lower wind speed values, while the E values are smaller for lower wind speeds.

While the effects of stability on the transfer coefficients were largest at high $|\zeta|$, large latent heat flux values occurred when the stability parameter (ζ) converged to zero due to the high wind speed effect (Fig. 8(d)). When the sensible and latent heat fluxes from a water surface are high, the water surface temperature is generally low. As the changes in the transfer coefficients cancel out by dividing the sensible heat flux by the latent heat flux, the stability condition of the atmospheric boundary layer does not impact the Bowen ratio (dimensionless). Bowen Ratio (β) values in the study period varied in the range of [–0.4, 0.3]. These low values of Bowen ratios show that most of the heat from the water surface was released by the evaporative fluxes. However, in the study lake, sensible heat fluxes must be taken into account in the total heat fluxes from the water surface due to the effect of sensible heat fluxes on atmospheric stability conditions.

Using the method developed in this study, considering the effect of atmospheric stability conditions, the sensible and latent heat fluxes from the (small) water surface were calculated and are shown in Figures 9 and 10. To show the effects of time scales on the results (especially in evaluating the performance of the model), hourly and daily averaged heat fluxes are illustrated in Figures 9 and 10, respectively. In addition, for both time scales, the heat fluxes with and without consideration of the atmospheric stability conditions are presented. As shown in both Figures 9 and 10, the effects of stability conditions on sensible heat fluxes are less than those on the latent heat flux values. However, the sensible heat flux values are smaller than the latent heat fluxes, so they cannot be ignored. Regarding the framework of the model as shown in Figure 3, to estimate the atmospheric stability conditions, the sensible heat flux values are needed (e.g. Equation (13)). Therefore, to consider the effect of stability conditions on heat fluxes from the water surface (especially for evaporative fluxes), sensible heat fluxes should be calculated accurately.

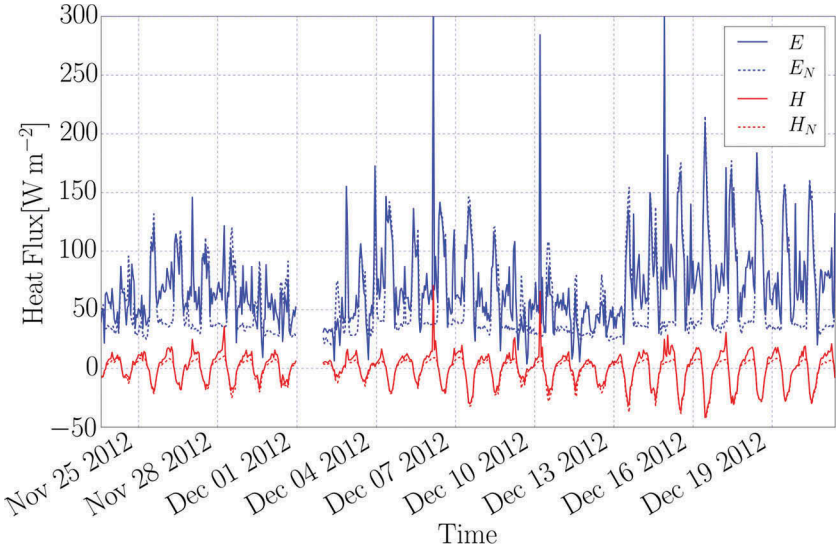

Figure 9. Calculated hourly averaged heat fluxes from Lake Binaba using proposed approach. Index *N*, indicates heat fluxes without considering the effects of atmospheric stability conditions on fluxes. Discontinuity in the graphs is due to malfunction of the weather station during these times.

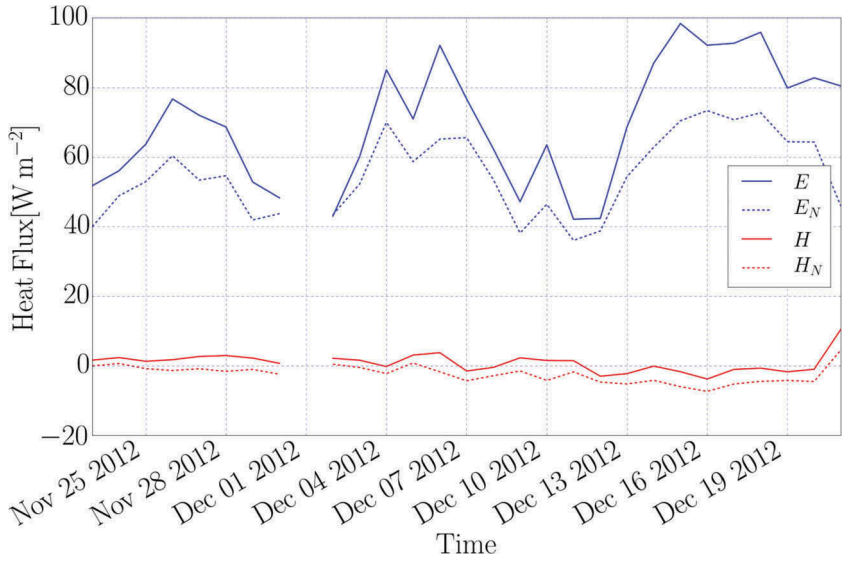

Figure 10. Calculated daily averaged heat fluxes from Lake Binaba using proposed approach with and without (*N*) consideration of the effects of atmospheric stability conditions on heat fluxes .

During the study period, the actual (considering the stability conditions) and neutral (assumption of natural atmospheric stability conditions) daily averaged evaporation values from the water surface were 2.5 mm d^{-1} (or 69.6 W m^{-2}) and 2.0 mm d^{-1} (55.6 W m^{-2}), respectively. The corresponding values for sensible heat flux were 0.65 and –2.6 W m^{-2}, respectively (Fig. 10).

Following the concept of the mass transfer method (Equations (1) and (2)) used in this study, the correlation of the sensible heat flux (H) with the product of wind speed (U_2) and difference in water surface temperature and air temperature ($\Delta T = T_{ws} - T_a$) was investigated. As shown in Figure 11(a), H is well correlated with $U_2(T_{ws} - T_a)$. This correlation can be described by the heat transfer coefficient (C_H), as shown in Equation (1). This correlation for $U_2(T_{ws} - T_a) \leq 0$ (where $T_{ws} < T_a$ and mostly stable conditions) seems to be linear. However, for $U_2(T_{ws} - T_a) > 0$ and for $T_{ws} > T_a$ (in unstable conditions), the correlation seems to be nonlinear. Therefore, for sensible heat flux from small water surfaces the heat transfer coefficient (C_H) can be approximated as a linear function for stable conditions, whereas this transfer coefficient is nonlinear for unstable conditions and should be calculated carefully. In addition, due to the small wind speed values at the study site, the term $U_2(T_{ws} - T_a)$ is dominated by changes in T_a and, therefore, its values must be collected accurately. Similar correlation analysis was executed for the values of E and $U_2(e_s - e_a)$. As shown in Figure 11(b) the correlation of latent heat flux (E) with $U_2(e_s - e_a)$ is more complex than the correlation of H and $U_2(T_{ws} - T_a)$ explained above. For large values of $U_2(e_s - e_a)$ (i.e. $U_2(e_s - e_a) \geq 2.0$) the relationship can be assumed to be linear, whereas for small values (i.e. $U_2(e_s - e_a) < 2.0$) the relationship is mostly nonlinear. This means that using a single water vapour transfer coefficient (or mass transfer coefficient, commonly referred to as the wind function) for all wind speeds to estimate latent heat fluxes from

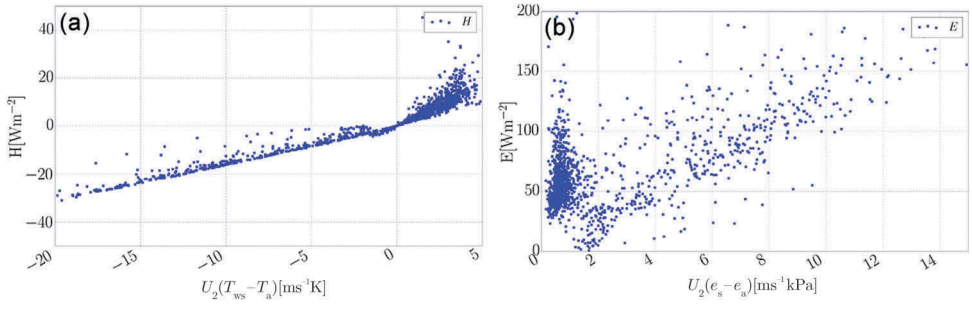

Figure 11. (a) Calculated sensible heat flux from water surface as a function of $U_2(T_{ws} - T_a)$; (b) calculated latent heat flux as a function of $U_2(e_s - e_a)$.

water surfaces could generate large errors in the calculated values, especially for water bodies when the wind speeds are low ($U_2 < 1.0$ m s^{-1}). As a conclusion from these analyses, for small water surfaces with low wind speeds the wind function (which is commonly used in mass transfer methods to estimate evaporation from water surfaces) can be justified for free convection situations. As this issue is beyond the aims of this study the reader is referred to the literature, for example Sill (1983), Huang (2002) and Edson *et al.* (2007), for more details.

9 Conclusions

The atmospheric stability conditions over small shallow lakes in arid and semi-arid regions have been shown to be important in estimating evaporation from open water bodies. In the model developed here, only standard micrometeorological parameters measured over the land are required to estimate heat fluxes from the water surface considering the atmospheric stability conditions. Using the Monin-Obukhov similarity theory (MOST), stability conditions were used to estimate latent and sensible heat fluxes. The bulk aerodynamic transfer method was improved by using the stability parameter from MOST and the atmospheric stability adjusted transfer coefficients. From the modelling results, atmospheric instability occurred more than 72.5% of the time in the study period, enhancing evaporation from the water surface by 44.7% on average. Using the developed method, the calculated daily average evaporation from Lake Binaba during the study period was 2.5 mm d^{-1}. The effects of atmospheric instability on the drag coefficient and heat (or water vapour) transfer coefficient were found to be 23.9% and 48.3%, respectively. The correlation of the computed sensible heat fluxes with the measured values was satisfactory, especially for the unstable atmosphere. Analysing the sensible and latent heat fluxes from Lake Binaba showed that air temperature was the dominant microclimatic variable for the sensible heat flux, whereas the latent heat flux (evaporation) was controlled by the vapour pressure of the overlying air for moderate to high wind speeds. For low wind speeds, estimation of the latent heat flux needs to take into account the free convection concept. For small water surfaces with low to moderate wind speeds, considering the free convection conditions should improve the heat flux estimation.

Acknowledgements

This work was carried out on Dutch national e-infrastructure with the support of the SURF Foundation (under grant number e-infra140092). The work was also supported by the Challenge Programme on Water and Food (CPWF) and the European Space Agency's TIGER.

Disclosure statement

No potential conflict of interest was reported by the authors.

ORCID

Ali Abbasi http://orcid.org/0000-0001-7098-3717

References

Ali, S., Ghosh, N.C., and Singh, R., 2008. Evaluating best evaporation estimate model for water surface evaporation in semi-arid region, India. *Hydrological Processes*, 22 (2), 1093–1106. doi:10.1002/hyp.6664

Ali, S., *et al.*, 2015. Simulation of water temperature in a small pond using parametric statistical models: implications of climate warming. *Journal of Environmental Engineering*, 142 (3), 1–13.

Amorocho, J. and DeVries, J., 1980. A new evaluation of the wind stress coefficient over water surfaces. *Journal of Geophysical Research*, 85 (C1), 433–442. doi:10.1029/JC085iC01p00433

Annor, F.O., *et al.*, 2009. Delineation of small reservoirs using radar imagery in a semi-arid environment: a case study in the upper east region of Ghana. *Physics and Chemistry of the Earth*, 34 (4–5), 309–315. doi:10.1016/j.pce.2008.08.005

Annor, F.O., *et al.*, 2016. Flux measurements over small lakes in Ghana's Upper East Region. *Advances in Water Resources* (manuscript submitted for publication).

Assouline, S., *et al.*, 2008. Evaporation from three water bodies of different sizes and climates: measurements and scaling analysis. *Advances in Water Resources*, 31 (1), 160–172. doi:10.1016/j.advwatres.2007.07.003

Barthlott, C., *et al.*, 2007. Long-term study of coherent structures in the atmospheric surface layer. *Boundary-Layer Meteorology*, 125 (1), 1–24. doi:10.1007/s10546-007-9190-9

Blanken, P.D., *et al.*, 2000. Eddy covariance measurements of evaporation from Great Slave Lake, Northwest Territories, Canada. *Water Resources Research*, 36 (4), 1069–1077. doi:10.1029/1999WR900338

Brutsaert, W., 1982. *Evaporation into the atmosphere: theory, history, and applications*. Dordrecht: Springer Netherlands.

Businger, J.A., *et al.*, 1971. Flux-profile relationships in the atmospheric surface layer. *Journal of the Atmospheric Sciences*, 28, 181–189. doi:10.1175/1520-0469(1971)028<0181:FPRITA>2.0.CO;2

Croley, T.E., 1989. Verifiable evaporation modelling on the Laurentian Great Lakes. *Water Resources Research*, 25 (5), 781–792. doi:10.1029/WR025i005p00781

Delclaux, F., Coudrain, A., and Condom, T., 2007. Evaporation estimation on Lake Titicaca: a synthesis review and modelling. *Hydrological Processes*, 21, 1664–1677. doi:10.1002/(ISSN)1099-1085

Derecki, J.A., 1981. Stability effects on great lakes evaporation. *Journal of Great Lakes Research*, 7 (4), 357–362. doi:10.1016/S0380-1330(81)72064-1

Dingman, S.L., 2002. *Physical hydrology*. 2nd ed. Upper Saddle River, NJ: Prentice-Hall.

Dyer, A.J., 1967. The turbulent transport of heat and water vapour in an unstable atmosphere. *Quarterly Journal of the Royal Meteorological Society*, 93 (398), 501–508. doi:10.1002/(ISSN)1477-870X

Edson, J., *et al*., 2007. The coupled boundary layers and air–sea transfer experiment in low winds. *Bulletin of the American Meteorological Society*, 88, 341–356. doi:10.1175/BAMS-88-3-341

Elbers, J., 2016. Introduction Alteddy [online]. Available from: http://www.climatexchange.nl/projects/alteddy/ [Accessed 10 Nov 2016].

Elbers, J.A., 2002. *Eddy correlation system Altera; User manuel*. Wageningen: Altera.

Fairall, C.W., Bradley, E.F., and Rogers, D.P., 1996. Bulk parameterization of air-sea fluxes for Tropical Ocean-Global Atmosphere Coupled-Ocean Atmosphere Response. *Journal of Geophysical Research*, 101 (C2), 3747–3764. doi:10.1029/95JC03205

Finch, J. and Calver, A., 2008. *Methods for the quantification of evaporation from lakes*. Wallingford: The World Meteorological Organization's Commission for Hydrology, Report.

Fowe, T., *et al*., 2015. Water balance of small reservoirs in the Volta basin a case study of Boura reservoir in Burkina Faso. *Agricultural Water Management*, 152, 99–109. doi:10.1016/j.agwat.2015.01.006

Fu, G., Charles, S.P., and Yu, J., 2009. A critical overview of pan evaporation trends over the last 50 years. *Climatic Change*, 97 (1–2), 193–214. doi:10.1007/s10584-009-9579-1

Fu, G., *et al*., 2004. Investigating the conversion coefficients for free water surface evaporation of different evaporation pans. *Hydrological Processes*, 18 (12), 2247–2262. doi:10.1002/(ISSN)1099-1085

Gallego-Elvira, B., *et al*., 2012. Evaluation of evaporation estimation methods for a covered reservoir in a semi-arid climate (south-eastern Spain). *Journal of Hydrology*, 458–459, 59–67. doi:10.1016/j.jhydrol.2012.06.035

Gianniou, S. and Antonopoulos, V., 2007. Evaporation and energy budget in Lake Vegoritis, Greece. *Journal of Hydrology*, 345 (3–4), 212–223. doi:10.1016/j.jhydrol.2007.08.007

Gokbulak, F. and Ozhan, S., 2006. Water loss through evaporation from water surfaces of lakes and reservoirs in Turkey. *E-WAter*, 2006, 1–6.

Henderson-Sellers, B., 1986. Calculating the surface energy balance for lake and reservoir modelling: a review. *Reviews of Geophysics*, 24 (3), 625–649. doi:10.1029/RG024i003p00625

Hicks, B., 1975. A procedure for the formulation of bulk transfer coefficients over water. *Boundary-Layer Meteorology*, 8 (3), 515–524. doi:10.1007/BF02153568

Huang, C.H., 2003. Modification of the Charnock wind stress formula to include the effects of free convection and swell. *In*: S. Jones, ed. *Advanced methods for practical applications in fluid mechanics*. InTech: Page, 47–71 [online]. Available from: http://www.intechopen.com/books/advanced-methods-for-practical-applications-in-fluid-mechanics/modification-of-the-charnock-wind-stress-formula-to-include-the-effects-of-free-convection-and-swell [Accessed 10 Nov 2016].

Keller, A., Sakthivadivel, R., and Seckler, D., 2000. *Water scarcity and the role of storage in development*. Colombo: International Water Management Institute, Research Report.

Kljun, N., *et al*., 2015. A simple two-dimensional parameterisation for Flux Footprint Prediction (FFP). *Geoscientific Model Development*, 8, 3695–3713. doi:10.5194/gmd-8-3695-2015

Legates, D.R. and McCabe Jr., G.J., 1999. Evaluating the use of 'goodness-of-fit' measures in hydrologic and hydroclimatic model validation. *Water Resources Research*, 35 (1), 233–241. doi:10.1029/1998WR900018

Liebe, J.R., 2009. *Hydrology of small reservoirs in semi-arid Northern Ghana*. Thesis (PhD). Cornell University.

Liebe, J.R., *et al*., 2009. Determining watershed response in data poor environments with remotely sensed small reservoirs as runoff gauges. *Water Resources Research*, 45 (7), 1–12. doi:10.1029/2008WR007369

Martínez-Granados, D., *et al*., 2011. The economic impact of water evaporation losses from water reservoirs in the Segura Basin, SE Spain. *Water Resources Management*, 25, 3153–3175. doi:10.1007/s11269-011-9850-x

McGloin, R., *et al*., 2014a. Modelling sub-daily evaporation from a small reservoir. *Journal of Hydrology*, 519, 2301–2311. doi:10.1016/j.jhydrol.2014.10.032

McGloin, R., *et al*., 2014b. Quantification of surface energy fluxes from a small water body using scintillometry and eddy covariance. *Water Resources Research*, 50, 494–513. doi:10.1002/wrcr.v50.1

Monin, A.S. and Obukhov, A.M., 1959. Basic laws of turbulent mixing in the surface layer of the atmosphere. *Tr Akad Nauk SSSR Geophiz Institute*, 24 (151), 163–187.

Monteith, J.L. and Unsworth, M.H., 2008. *Principles of environmental physics*. 3rd ed. Oxford: Elsevier.

Mugabe, F., Hodnett, M.G., and Senzanje, A., 2003. Opportunities for increasing productive water use from dam water: a case study from semi-arid Zimbabwe. *Agricultural Water Management*, 62 (2), 149–163. doi:10.1016/S0378-3774(03)00077-5

Poussin, J.-C., *et al*., 2015. Performance of small reservoir irrigated schemes in the Upper Volta basin: case studies in Burkina Faso and Ghana. *Water Resources and Rural Development*, 6, 50–65. doi:10.1016/j.wrr.2015.05.001

Renfrew, I.A., *et al*., 2002. A comparison of surface layer and surface turbulent flux observations over the Labrador Sea with ECMWF analyses and NCEP reanalyses. *Journal of Physical Oceanography*, 32, 383–400. doi:10.1175/1520-0485(2002)032<0383:ACOSLA>2.0.CO;2

Rosenberry, D., *et al*., 2007. Comparison of 15 evaporation methods applied to a small mountain lake in the northeastern USA. *Journal of Hydrology*, 340 (3–4), 149–166. doi:10.1016/j.jhydrol.2007.03.018

Rouse, W.R.W.R., *et al*., 2003. Interannual and seasonal variability of the surface energy balance and temperature of Central Great Slave Lake. *Journal of Hydrometeorology*, 4 (4), 720–730. doi:10.1175/1525-7541(2003)004<0720:IASVOT>2.0.CO;2

Sartori, E., 2000. A critical review on equations employed for the calculation of the evaporation rate from free water

surfaces. *Solar Energy*, 68 (1), 77–89. doi:10.1016/S0038-092X(99)00054-7

Schertzer, W.M., *et al.*, 2003. Over-lake meteorology and estimated bulk heat exchange of Great Slave Lake in 1998 and 1999. *Journal of Hydrometeorology*, 4 (4), 649–659. doi:10.1175/1525-7541(2003)004<0649:OMAEBH>2.0.CO;2

Sill, B.L., 1983. Free and forced convection effects on evaporation. *Journal of Hydraulic Engineering*, 109 (9), 1216–1231. doi:10.1061/(ASCE)0733-9429(1983)109:9(1216)

Singh, V.P. and Xu, C.-Y., 1997a. Sensitivity of mass transfer-based evaporation equations to errors in daily and monthly input data. *Hydrological Processes*, 11, 1465–1473. doi:10.1002/(ISSN)1099-1085

Singh, V.P. and Xu, C.-Y., 1997b. Evaluation and generalization of 13 mass transfer equations for determining free water evaporation. *Hydrological Processes*, 11 (3), 311–323. doi:10.1002/(ISSN)1099-1085

Smith, S.D., 1988. Coefficients for sea surface wind stress, heat flux, and wind profiles as a function of wind speed and temperature. *Journal of Geophysical Research*, 93 (15), 15467–15472. doi:10.1029/JC093iC12p15467

Stannard, D. and Rosenberry, D., 1991. A comparison of short-term measurements of lake evaporation using eddy correlation and energy budget methods. *Journal of Hydrology*, 122 (1–4), 15–22. doi:10.1016/0022-1694(91)90168-H

Stull, R.B., 1988. *An introduction to boundary layer meteorology*. 1st ed. Dordrecht: Springer Netherlands.

van Emmerik, T.H.M., *et al.*, 2013. Measuring heat balance residual at lake surface using distributed temperature sensing. *Limnology and Oceanography: Methods*, 11 (1991), 79–90. doi:10.4319/lom.2013.11.79

Verburg, P. and Antenucci, J.P., 2010. Persistent unstable atmospheric boundary layer enhances sensible and latent heat loss in a tropical great lake: lake Tanganyika. *Journal of Geophysical Research*, 115, 1–13. doi:10.1029/2009JD012839

Vercauteren, N., 2011. *Water vapour and heat exchange over lakes*. Thesis (PhD). École Ploythechnique Federale de Lausanne.

Vesala, T., *et al.*, 2008. Flux and concentration footprint modelling: state of the art. *Environmental Pollution*, 152 (3), 653–666. doi:10.1016/j.envpol.2007.06.070

Vidal-López, P., *et al.*, 2012. Determination of synthetic wind functions for estimating open water evaporation with Computational Fluid Dynamics. *Hydrological Processes*, 26, 3945–3952. doi:10.1002/hyp.v26.25

Vinnichenko, N.A., *et al.*, 2011. Study of evaporation from water reservoir. *22nd International Symposium on Transport Phenomena*, 8-11 Nov. Delft: Delft University of Technology, 1–11.

Xu, C.-Y. and Singh, V.P., 2000. Evaluation and generalization of radiation-based methods for calculating evaporation. *Hydrological Processes*, 14 (2), 339–349. doi:10.1002/(ISSN)1099-1085

Xu, C.-Y. and Singh, V.P., 2001. Evaluation and generalization of temperature-based methods for calculating evaporation. *Hydrological Processes*, 15 (2), 305–319. doi:10.1002/(ISSN)1099-1085

Zeng, X., Zhao, M., and Dickinson, R., 1998. Intercomparison of bulk aerodynamic algorithms for the computation of sea surface fluxes using TOGA COARE and TAO data. *Journal of Climate*, 11, 2628–2644. doi:10.1175/1520-0442(1998)011<2628:IOBAAF>2.0.CO;2